ARTICLE

doi:10.1038/nature11116

Superallowed Gamow–Teller decay of the doubly magic nucleus ^{100}Sn

C. B. Hinke[1], M. Böhmer[1], P. Boutachkov[2], T. Faestermann[1], H. Geissel[2], J. Gerl[2], R. Gernhäuser[1], M. Górska[2], A. Gottardo[3], H. Grawe[2], J. L. Grębosz[4], R. Krücken[1,5], N. Kurz[2], Z. Liu[6], L. Maier[1], F. Nowacki[7], S. Pietri[2], Zs. Podolyák[8], K. Sieja[7], K. Steiger[1], K. Straub[1], H. Weick[2], H.-J. Wollersheim[2], P. J. Woods[6], N. Al-Dahan[8], N. Alkhomashi[8], A. Ataç[9], A. Blazhev[10], N. F. Braun[10], I. T. Čeliković[11], T. Davinson[6], I. Dillmann[2], C. Domingo-Pardo[12], P. C. Doornenbal[13], G. de France[14], G. F. Farrelly[8], F. Farinon[2], N. Goel[2], T. C. Habermann[2], R. Hoischen[2], R. Janik[15], M. Karny[16], A. Kaşkaş[9], I. M. Kojouharov[2], Th. Kröll[17], Y. Litvinov[2], S. Myalski[4], F. Nebel[1], S. Nishimura[13], C. Nociforo[2], J. Nyberg[18], A. R. Parikh[19], A. Procházka[2], P. H. Regan[8], C. Rigollet[20], H. Schaffner[2], C. Scheidenberger[2], S. Schwertel[1], P.-A. Söderström[13], S. J. Steer[8], A. Stolz[21] & P. Strmeň[15]

The shell structure of atomic nuclei is associated with 'magic numbers' and originates in the nearly independent motion of neutrons and protons in a mean potential generated by all nucleons. During β$^+$-decay, a proton transforms into a neutron in a previously not fully occupied orbital, emitting a positron–neutrino pair with either parallel or antiparallel spins, in a Gamow–Teller or Fermi transition, respectively. The transition probability, or strength, of a Gamow–Teller transition depends sensitively on the underlying shell structure and is usually distributed among many states in the neighbouring nucleus. Here we report measurements of the half-life and decay energy for the decay of ^{100}Sn, the heaviest doubly magic nucleus with equal numbers of protons and neutrons. In the β-decay of ^{100}Sn, a large fraction of the strength is observable because of the large decay energy. We determine the largest Gamow–Teller strength so far measured in allowed nuclear β-decay, establishing the 'superallowed' nature of this Gamow–Teller transition. The large strength and the low-energy states in the daughter nucleus, ^{100}In, are well reproduced by modern, large-scale shell model calculations.

Gamow–Teller transitions, in which a proton is transformed into a neutron or vice versa, while possibly flipping its spin, represent an important spin–isospin degree of freedom in atomic nuclei. They are important in many astrophysical processes: they govern, for example, electron capture during the core collapse of supernovae. Furthermore, a detailed understanding of Gamow–Teller transitions will provide an essential constraint on the neutrino mass, in the event that neutrinoless double β-decay is ever observed. Most of the Gamow–Teller strength is found in the collective Gamow–Teller giant resonance (GTGR) of the neighbouring nucleus, which is typically a broad structure composed of many states. Whereas in charge-exchange reactions in stable nuclei the full GTGR is accessible, the Gamow–Teller strength in unstable nuclei can, so far, only be studied through β-decay. However, β-decay studies can observe only the fraction of the total Gamow–Teller strength within the decay energy window. Towards more proton-rich nuclei, this window becomes larger. Nevertheless, it is still experimentally challenging to detect all small components of the Gamow–Teller strength[1,2]. Thus, in most nuclei, measuring the full Gamow–Teller strength is difficult because it is fragmented and only partly accessible in β-decays.

^{100}Sn has $N = 50$ neutrons and $Z = 50$ protons, and as a result has completely occupied shells. It is therefore called 'doubly magic' and is particularly suited both experimentally and theoretically to the study of Gamow–Teller transitions. The closed $N = Z = 50$ shells reduce the effect of long-range correlations, thus decreasing the amount of fragmentation of the GTGR. Theoretical predictions suggest that a single state is dominantly populated in this decay. At the same time, the energy window for β-decay is ~7.4 MeV (ref. 3), and most of the GTGR is therefore accessible. Such a situation for a doubly magic system is realized nowhere else in the Segrè chart (a two-dimensional lattice in which all known nuclei are arranged with N and Z on the x and y axes, respectively): ^{16}O and ^{40}Ca are stable nuclei; ^{56}Ni has too small a Q_{EC} value (the energy available for β$^+$-decay or electron-capture decay) to make the Gamow–Teller resonance observable in β-decay; and doubly magic nuclei with $N = Z$ that are heavier than ^{100}Sn are unbound. Also, a recent experiment shows that ^{56}Ni has a much more fragmented Gamow–Teller strength[4] as a result of a less robust $N = Z = 28$ doubly magic shell closure as well as subtle differences in the shell structure (Methods Summary and Supplementary Information).

In an extreme, pure single-particle picture, the only possible Gamow–Teller transition of ^{100}Sn is the decay of a proton in the completely filled $g_{9/2}$ shell to a neutron in the empty $g_{7/2}$ shell because the $g_{9/2}$ neutron orbital is filled and no levels above $Z = 50$ are occupied. The large energy separation (shell gap) between these spin-parallel ($g_{9/2}$) and spin-antiparallel ($g_{7/2}$) orbitals, for which the orbital angular momentum is $L = 4$, is responsible for 50 being a magic number. The β-decay of ^{100}Sn is supposed to be enhanced as a result of the large

[1]Physik Department E12, Technische Universität München, D-85748 Garching, Germany. [2]GSI Helmholtzzentrum für Schwerionenforschung GmbH, D-64291 Darmstadt, Germany. [3]Istituto Nazionale di Fisica Nucleare, Laboratori Nazionali di Legnaro, 35020 Legnaro, Italy. [4]The Henryk Niewodniczanski Institute of Nuclear Physics (IFJ PAN), 31-342 Krakow, Poland. [5]TRIUMF, Vancouver, British Columbia V6T 2A3, Canada. [6]School of Physics & Astronomy, The University of Edinburgh, Edinburgh EH9 3JZ, UK. [7]Université de Strasbourg, IPHC, 67037 Strasbourg Cedex, France. [8]Department of Physics, University of Surrey, Guildford GU2 7XH, UK. [9]Physics Department, Faculty of Science, Ankara University, 06100 Tandogan, Ankara, Turkey. [10]Institute of Nuclear Physics, University of Cologne, D-50937 Köln, Germany. [11]Institute Vinca, University of Belgrade, 11000 Belgrade, Serbia. [12]IFIC, CSIC-University of Valencia, E-46071 Valencia, Spain. [13]RIKEN Nishina Center, Wako, Saitama 351-0198, Japan. [14]Grand Accélérateur National d'Ions Lourds, CEA/DSM-CNRS/IN2P3, 14076 Caen, France. [15]Comenius University, 818 06 Bratislava 16, Slovakia. [16]Institute of Experimental Physics, University of Warsaw, PL-00681 Warsaw, Poland. [17]Institut für Kernphysik, Technische Universität Darmstadt, D-64289 Darmstadt, Germany. [18]Department of Physics & Astronomy, Uppsala University, SE-75120 Uppsala, Sweden. [19]Departamento de Fisica i Enginyeria Nuclear, Universitat Politecnica de Catalunya (EUETIB), E-08036 Barcelona, Spain. [20]KVI, University of Groningen, 9747AA Groningen, The Netherlands. [21]National Superconducting Cyclotron Laboratory, Michigan State University, East Lansing, Michigan 48824-1321, USA.

number of protons occupying the $g_{9/2}$ shell, which can decay to the mostly empty neutron $g_{7/2}$ shell. This would lead to a GTGR consisting of only a single $I^{\pi} = 1^{+}$ level (I, spin; π, parity) with a large Gamow–Teller strength of about $B_{GT} = 10$, taking into account the standard renormalization factor (0.75) of the Gamow–Teller matrix element due to configurations outside the model space[5]. This unique situation has been termed 'superallowed' Gamow–Teller decay[6]. Even in more realistic models, including particle–hole correlations, the Gamow–Teller decay of the ground state of ^{100}Sn is predicted to populate with more than 95% probability a single 1^{+} state in ^{100}In at an excitation energy of about 3 MeV. In these calculations, a Gamow–Teller strength of around 8–14 is obtained[7–10], leading to renormalized predictions of 5–7 (refs 8, 10). These theoretical results are summarized in Methods Summary and Supplementary Information.

The production of ^{100}Sn, and the study of its decay properties, has been the aim of several experiments[11–16], but in these only a few ^{100}Sn nuclei were uniquely identified. Here we report a new measurement of the half-life and Q_{EC} value from 259 identified ^{100}Sn nuclei, which yields the smallest log(ft) value of any known β-decay (here t is the half-life and f is a phase space factor that takes into account the trivial decay energy dependence of the half-life). The Gamow–Teller strength is inversely proportional to ft and thus is greatest for the ^{100}Sn decay establishing the robustness of $N = Z = 50$ shell closures. The experimentally observed Gamow–Teller strength is well described in modern, large-scale shell model (LSSM) calculations, which are able to handle an unprecedentedly large degree of configuration mixing in the case of ^{100}Sn. This ^{100}Sn doubly magic shell closure is the benchmark for various topics currently discussed in this mass region, such as spin-aligned pairing in $N = Z$ nuclei, alpha clustering and quadrupole collectivity in the Sn isotopic chain.

Experimental details

The experiment was performed at the GSI Helmholtzzentrum für Schwerionenforschung, Germany. A ^{124}Xe beam with a kinetic energy of 1.0A GeV (A, nucleon number) and 1-s-long spills of 3×10^9 ions every 3 s was directed onto a beryllium target placed in front of the fragment separator[17]. Neutron-deficient nuclei were produced through relativistic projectile fragmentation, transmitted to the final focal plane of the fragment separator, and identified event by event (Fig. 1). The correct identification was verified by observing the γ-radiation depopulating known isomers, for example the 8^{+} isomer in ^{98}Cd. In total, 259 ^{100}Sn nuclei were unambiguously identified.

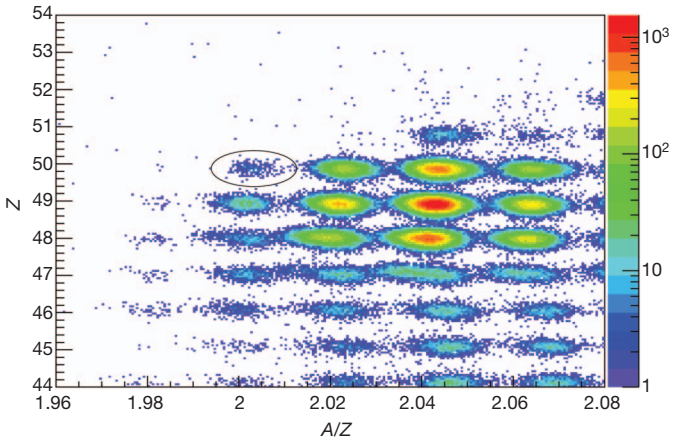

Figure 1 | Particle identification plot. Events are plotted with respect to Z and the mass-to-charge ratio, A/Z, for the full statistics of the ^{100}Sn fragment separator setting. In total, 259 ^{100}Sn nuclei (those indicated in the figure) were unambiguously identified. Resolutions (full-widths at half-maximum) in mass of $\Delta A = 0.32$ ($A = N + Z$) and in nuclear charge of $\Delta Z = 0.25$ were obtained. The colours indicate the number of events per bin in a logarithmic scale as indicated on the right-hand side.

This corresponds to a production rate of 0.75 per hour and a cross-section of 5.8 ± 2.1 pb. All uncertainties correspond to one standard deviation.

The ions were implanted into a stack of highly segmented silicon strip detectors surrounded by the RISING array, which consists of 105 germanium detectors arranged in the stopped-beam configuration[18] to detect γ-rays with high efficiency. Of the 259 identified ^{100}Sn nuclei, 163 were stopped in the 2.1-mm-thick implantation layer.

Analysis and results

Following a ^{100}Sn implantation in a pixel of the implantation zone of the silicon detector, all decay events were recorded that occurred within 15 s in that pixel or in the directly neighbouring ones. During this correlation time, it was possible to assign 126 decay chains to the 163 ^{100}Sn implantations. A maximum-likelihood (MLH) analysis with a maximum of three decay events during the correlation time was used to analyse these decay chains. The half-life of ^{100}Sn was deduced to be 1.16 ± 0.20 s in the MLH analysis using established values for the lifetimes of the daughter nuclei. The measurement is much more precise than previous experiments yielding $0.94^{+0.54}_{-0.27}$ s (ref. 14) and $0.55^{+0.70}_{-0.31}$ s (ref. 16). In Fig. 2, we show the decay curve for ^{100}Sn.

Figure 3 shows the γ-ray spectrum observed in coincidence with decay events following ^{100}Sn implantations. Notably, discrete γ-transitions from the ^{100}Sn decay could be observed. The five transitions denoted in Fig. 3 are associated with the depopulation of excited states in the daughter nucleus ^{100}In.

The statistics were sufficient only to establish a coincidence between the 436-keV and 96-keV transitions, and it is thus impossible to deduce an unambiguous level scheme for ^{100}In. Within the uncertainties, the transitions could have the same intensity, which would allow for a single cascade of five transitions from the excited 1^{+} state to the ground state. However, this would lead to an excitation energy of more than 4 MeV, which is higher than the value of about 2.5 MeV predicted with realistic shell model calculations (see, for example, refs 19, 20). The large uncertainties in the observed intensities also allow for two parallel cascades originating from this 1^{+} state.

Figure 4 shows the relevant level scheme for ^{100}In obtained from LSSM calculations. In this approach, ^{100}Sn is not treated as an inert, doubly magic core but instead excitations across the $N = Z = 50$ shell closures were allowed within the fifth ($4\hbar\omega$) harmonic oscillator shell (Methods Summary and Supplementary Information).

The states of two multiplets that are relevant for the decay are shown. The states originate in the coupling of proton (π) holes in the $g_{9/2}$ orbital either to neutron (ν) particles in the $g_{7/2}$ orbital ($\pi g_{9/2}^{-1} \otimes \nu g_{7/2}^{1}$) with total spin and parity $I^{\pi} = 1^{+}$–8^{+} or to neutron

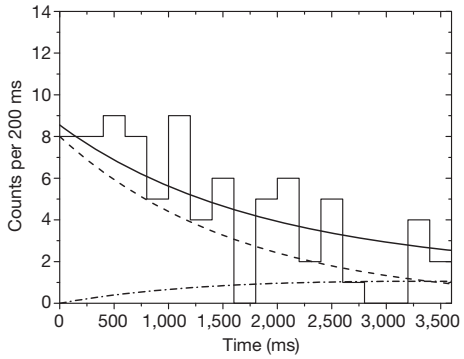

Figure 2 | Time distribution of first decay events. The histogram shows the observed time distribution of all first decay events in the nearest-neighbouring pixels after implantation of ^{100}Sn nuclei. Decay curves resulting from the MLH analysis are shown individually for ^{100}Sn (dashed) and its daughter nucleus ^{100}In (dash–dot). The solid line shows the sum of these decay curves and takes into account a small amount of random background.

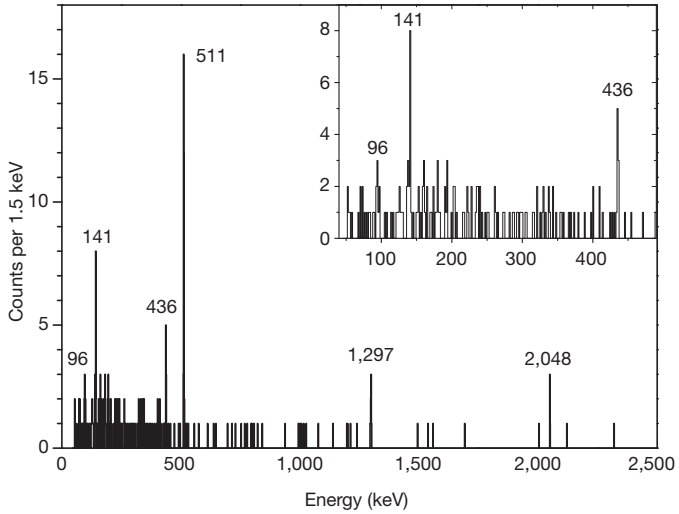

Figure 3 | Spectrum of γ-radiation. Energy distribution of the γ-radiation observed within 4 s after implantation of ^{100}Sn. With 65% probability these are directly following the ^{100}Sn decay. The other contributions are uncorrelated background decays and daughter decays of ^{100}In. None of the observed lines corresponds to known transitions from these minor contributions. The line at 511 keV is due to positron annihilation radiation. The measured absolute numbers of transitions of the five lines with the energies 96, 141, 436, 1,297 and 2,048 keV are respectively 79 ± 40, 100 ± 31, 59 ± 22, 72 ± 26 and 53 ± 26 corrected for electron conversion assuming M1 (magnetic dipole) transitions. Inset, enlarged view of the energy range up to 500 keV.

particles in the $d_{5/2}$ orbital ($\pi g_{9/2}^{-1} \otimes \nu d_{5/2}^{1}$) with $I^{\pi} = 2^{+}$–7^{+}. The predictions reflect the observed γ-ray transitions well if the high-energy, 2,048-keV, transition populates the lowest 2^{+} state, this then decays to lower-lying states via the 436-, 141- and 96-keV transitions, and the decay chain ends either in the 6^{+} ground state or a low-lying isomeric state with unobserved decay. In this picture, the second 2^{+} state is populated by the 1,297-keV transition and decays to the lower-lying 2^{+} and 3^{+} states. This may lead to a fragmentation of the intensities, making it impossible to observe these transitions in the present experiment. This picture is supported by three experimental facts: the measurement of the total γ-ray energy ($E^{*}_{1+} = 2.76 \pm 0.43$ MeV) in a previous experiment with a bismuth germanate detector[14]; the known mass difference between ^{100}Sn and ^{100}In[13], combined with our measured β-decay end-point energy ($E^{*}_{1+} = 2.6 \pm 1.0$ MeV); and our observation of a single event of β-delayed proton emission ($E^{*}_{1+} = 2.93 \pm 0.34$ MeV). It is fully consistent with the expectation that a single 1^{+} state is dominantly populated in the decay. Further details are given in Methods Summary and Supplementary Information.

As a key feature of this experiment, we measured the kinetic energy of the decay positrons fully absorbed in the compact silicon detector array. The spectrum resulting from the summed energies deposited by a β-particle in the pixels of the calorimeter up to 3 s after a ^{100}Sn implantation is shown in Fig. 5. It was fitted using a MLH analysis based on a single-component β-decay phase space function to determine the end-point energy in the decay of ^{100}Sn. For the fit of the end-point energy, only data in the energy region between 400 and 2,600 keV were used. In the analysis, corrections were applied to account for the emission of conversion electrons instead of low-energy γ-rays during the de-excitation of the daughter nucleus ^{100}In, for bremsstrahlung emitted when the positrons are slowed down and for the annihilation of positrons in flight before the deposition of their total kinetic energy. The end-point energy of the β-decay, if populating a single final state in the daughter nucleus ^{100}In, was determined to be 3.29 ± 0.20 MeV. The corresponding fraction of electron-capture decays is 13% of all ^{100}Sn decays.

Discussion

Using the measured half-life and the end-point energy, we calculated a log(*ft*) value of $2.62^{+0.13}_{-0.11}$, which is the smallest such value found so far for any nuclear β-decay. Thus, the Gamow–Teller decay of ^{100}Sn has a much larger strength than the known $0^{+} \rightarrow 0^{+}$ superallowed Fermi decays of $N = Z$ nuclei and can indeed be considered a superallowed Gamow–Teller decay[21]. This finding is also illustrated in Fig. 6, which shows the distribution of log(*ft*) values for allowed Gamow–Teller and Fermi transitions.

The extracted Gamow–Teller strength of the ^{100}Sn ground-state decay to the single excited 1^{+} state in ^{100}In is $B_{GT} = 9.1^{+2.6}_{-3.0}$. The measured value is extraordinarily large but consistent with the value of $B_{GT} = 5.8^{+5.5}_{-3.2}$ deduced from previous results for Q_{EC} and half-life[22], within the large error bars of the earlier measurement. The uncertainty in the new B_{GT} value is dominated by the uncertainty in the β-decay end-point energy. The extraction of the strength was done under the assumption that the Gamow–Teller decay was into only one final 1^{+}

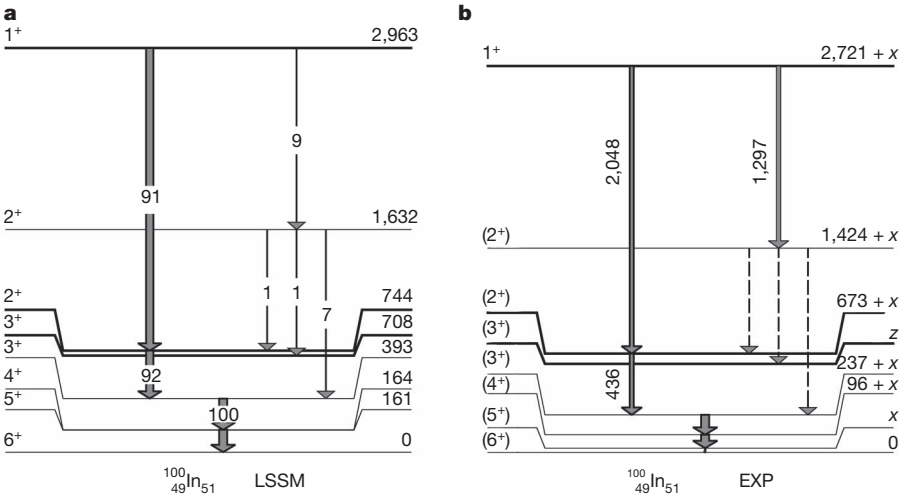

Figure 4 | Tentative level scheme of ^{100}In. **a**, LSSM calculation of the low-lying excited states in ^{100}In. Spin and parity (I^{π}) are shown on the left and energy (keV) is shown on the right. Populated levels with an almost pure $\pi g_{9/2}^{-1} \otimes \nu g_{7/2}^{1}$ configuration are indicated with bold lines, and the remaining levels are part of the $\pi g_{9/2}^{-1} \otimes \nu d_{5/2}^{1}$ multiplet. Gamma-transitions with their relative intensities (in per cent and indicated by arrow width) are shown for selected transitions. **b**, Most likely level scheme for the five observed γ-transitions in ^{100}In (three with energies (keV) shown). Because one low-energy transition might have been missed, the energy of the levels might have a systematic shift of up to $x = 80$ keV. The dashed transitions and level *z* were not observed. The assignment of spin and parity is certain only for the 1^{+} state; the others are tentative assignments based on theory.

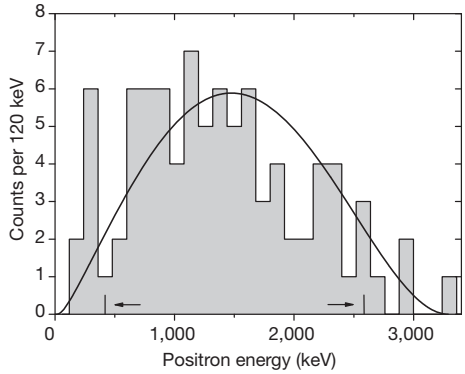

Figure 5 | Distribution of the positron energies emitted in the β-decay of ^{100}Sn. The spectrum contains only decay events that can be assigned to ^{100}Sn decays with a probability of at least 75%. The MLH fit was applied to the region between 400 and 2,600 keV, which is indicated with markers. The solid curve illustrates the shape of the best-fitting single-component β-decay phase space function determined by MLH analysis.

state in ^{100}In. However, if 1^+ states at excitation energies above the observed state were also populated, the summed Gamow–Teller strength would increase while the strength of the decay into the first excited 1^+ state would decrease. It would have been difficult to observe such higher-energy states because the reduced phase space for lower-energy β^+-particles would have led to a strongly reduced population.

The LSSM calculations, which within the *gds* harmonic oscillator shell take into account most of the long-range correlations across the $N = Z = 50$ doubly magic shell closure and include up to five particle–hole excitations (Methods Summary and Supplementary Information), yield a total summed Gamow–Teller strength of $B_{GT} = 8.19$ for all possible final states in the daughter nucleus up to 60 MeV. The standard renormalization due to correlations beyond the 0*g*, 1*d*, 2*s* model space has been applied[5]. The distribution of strength up to an excitation energy of 10 MeV is shown in Methods Summary and Supplementary Fig. 1.

A Gamow–Teller strength of $B_{GT} = 7.82$ is predicted in the experimental Q_{EC} window of 7.03(20) MeV. This corresponds to a reduction in the total renormalized Gamow–Teller strength of the extreme single-particle estimate ($B_{GT,ESPM} \approx 10$) by 18% for excitation energies up to 60 MeV and by 22% in the Q_{EC} window. It is due to mixing in the *gds* harmonic oscillator shell, that is, emptying of the proton $g_{9/2}$ orbital, pre-filling of the neutron $g_{7/2}$ orbital and destructive interference of the four possible combinations of Gamow–Teller transitions within the *g* orbital ($L = 4$). The occupation numbers of the two orbitals that are linked by the Gamow–Teller operator, which acts on spin and isospin but does not change *L*, directly influence the strength of the transition matrix element.

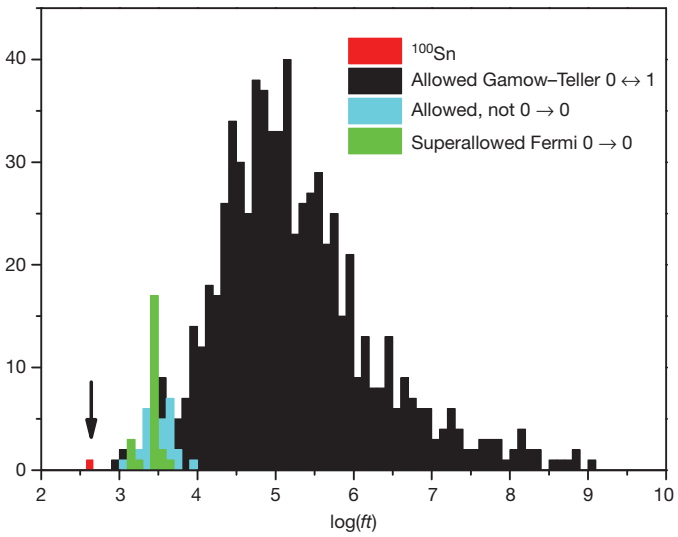

Figure 6 | Log(*ft*) values of allowed nuclear β-decays. Number distribution of log(*ft*) values for allowed β-transitions (obeying the selection rules). The data are from ref. 26. The values are for generally allowed Gamow–Teller transitions between 0^+ and 1^+ states (black), mixed Fermi/Gamow–Teller transitions (blue) and the well-established pure, superallowed Fermi transitions from 0^+ to 0^+ states (green). The decay of ^{100}Sn is unique because it has the smallest known log(*ft*) value (red) of any nuclear β-decay.

The calculation predicts that the largest fraction of the strength remains located in the first excited 1^+ state, in agreement with earlier calculations[7,21]. Nevertheless, according to our LSSM calculations it is reasonable to consider that several 1^+ states in ^{100}In are populated in the decay of ^{100}Sn. If, as an exercise, we take from the LSSM calculation the four lowest 1^+ states in ^{100}In with their energy splittings and relative Gamow–Teller strengths (Methods Summary and Supplementary Information), the value of $B_{GT}(1_1^+) = 9.1^{+2.6}_{-3.0}$ (assuming a single 1^+ state) would be reduced to $B_{GT}(1_1^+) = 7.6^{+2.2}_{-2.5}$ for the first excited 1^+ state using the experimental half-life and β-spectrum. The corresponding summed Gamow–Teller strength would be $\sum_{i=1}^{4} B_{GT}(1_1^+) = 9.9^{+2.8}_{-3.2}$. Because this exercise served only to gauge the effect of branching on the experimental B_{GT} value, no error for the branching ratios is included.

The LSSM result of $B_{GT} = 5.7$ for this first excited 1^+ state agrees within the statistical uncertainty with the value, $B_{GT} = 7.6^{+2.2}_{-2.5}$, extracted from the experimental log(*ft*) value under the above assumptions. The experimental concentration of most of the Gamow–Teller strength in the first excited 1^+ state clearly classifies the ^{100}Sn Gamow–Teller decay as superallowed. This large experimental Gamow–Teller strength of the transition to the first excited 1^+ state proves that both the ^{100}Sn ground state and the first excited 1^+ state in ^{100}In have relatively pure wavefunctions. As expected, the LSSM calculation reveals that the respective wavefunctions consist predominantly of the $\pi g_{9/2}^{10} \otimes \nu g_{7/2}^{0}$ (82% probability) and $\pi g_{9/2}^{9} \otimes \nu g_{7/2}^{1}$ (54% probability) components. The high purity of the wavefunctions within the *gds* model space establishes the simultaneous robustness of the $Z = 50$ and $N = 50$ shell closures in ^{100}Sn, which is only ~3 MeV from the proton drip line, corroborating for $N = 50$ the results of refs 23, 24, and excludes the need for explicitly treating the unbound proton orbits as continuum states.

The LSSM calculations allow enough configuration mixing in the *gds* shell that convergent results are obtained, leading to meaningful conclusions in this exotic region far from the valley of stability. This indicates that it should be possible to obtain reliable, more accurate results for nuclei in the neighbourhood of ^{100}Sn, especially close to the proton drip line.

The underlying shell structures of nuclei in the vicinity of ^{100}Sn have to be determined with the highest possible accuracy to address the important issues in nuclear structure, such as the possibility of a new coupling scheme developing in the $N = Z$ nuclei in the vicinity of ^{100}Sn (ref. 25). The present measurement is a stringent test for LSSM calculations, in which the realistic character of such a coupling scheme still needs to be probed.

A better understanding of the nuclear structure is of major importance for modelling weak interaction rates in nuclei, which depend on the underlying shell structure and are important in many astrophysical processes. For example, Gamow–Teller transitions govern electron capture during the core collapse of supernovae. Also, Gamow–Teller transitions are an essential constraint on the theoretical calculations of neutrino-less double-β-decay matrix elements, the knowledge of which is necessary to relate the neutrino mass to the rate of this yet undiscovered process. Further interest in the decay rates of nuclei around ^{100}Sn comes from the study of certain astrophysical processes, as this region has been considered the end of the rapid proton capture process due to the Sn-Sb-Te cycle.

METHODS SUMMARY

^{100}Sn and neighbouring nuclei were produced by fragmentation of a 1.0A-GeV ^{124}Xe beam from the GSI accelerators, separated in the fragment separator and identified by multiple energy-loss, magnetic rigidity and time-of-flight measurements. The nuclei were stopped in an implantation detector with high spatial resolution to correlate implantations with succeeding decays. The device was surrounded by the stopped-beam RISING array of 15×7 germanium detectors in close geometry. In this configuration, the set-up enabled us to do nearly 4π spectroscopy of the emitted γ-radiation and particle-decay radiation. With a photopeak efficiency of about 10% (1 MeV) for γ-ray detection and nearly 100% for full energy detection of decay particles up to 5 MeV, this high-resolution set-up allowed for a maximum use of the secondary beam.

The ^{100}Sn half-life and the β-decay end-point energy were calculated in the framework of a MLH analysis applied respectively to the time distribution of β-decays after implantation and the energy distribution of emitted positrons. This analysis also considered the daughter decays and the presence of uncorrelated random background decays from previous implantations.

To interpret the measured Gamow–Teller strength and the observed γ-rays emitted from ^{100}In, we carried out LSSM calculations. The valence space used in the LSSM consists of the fifth ($4\hbar\omega$) harmonic oscillator shell, that is, proton and neutron $\pi\nu(g,d,s)$ orbitals outside the ^{80}Zr core. The calculations included up to five particle–hole excitations from the $g_{9/2}$ proton and neutron orbitals to the rest of the shell, which made it possible for us to obtain convergent results for excitation spectra and the Gamow–Teller strength.

Received 28 October 2011; accepted 2 April 2012.

1. Ichimura, M., Sakai, H. & Wakasa, T. Spin-isospin responses via (p,n) and (n,p) reactions. *Prog. Part. Nucl. Phys.* **56,** 446–531 (2006).
2. Hardy, J. C., Carraz, L. C., Jonson, B. & Hansen, P. G. The essential decay of pandemonium: a demonstration of errors in complex beta-decay schemes. *Phys. Lett. B* **71,** 307–310 (1977).
3. Audi, G., Wapstra, A. H. & Thibault, C. The Ame2003 atomic mass evaluation: (II). Tables, graphs and references. *Nucl. Phys. A* **729,** 337–676 (2003).
4. Sasano, M. *et al.* Gamow-Teller transition strengths from ^{56}Ni. *Phys. Rev. Lett.* **107,** 202501 (2011).
5. Caurier, E., Martínez-Pinedo, G., Nowacki, F., Poves, A. & Zuker, P. A. The shell model as a unified view of nuclear structure. *Rev. Mod. Phys.* **77,** 427–488 (2005).
6. Brown, B. A. The nuclear shell model towards the drip lines. *Prog. Part. Nucl. Phys.* **47,** 517–599 (2001).
7. Brown, B. A. & Rykaczewski, K. Gamow-Teller strength in the region of ^{100}Sn. *Phys. Rev. C* **50,** R2270–R2273 (1994).
8. Dean, D. J., Koonin, S. E., Kuo, T. T. S., Langanke, K. & Radha, P. B. Complete $0\hbar\omega$ shell model Monte Carlo calculations of ^{94}Ru, ^{96}Pd, ^{96,98}Cd and ^{100}Sn. *Phys. Lett. B* **367,** 17–20 (1996).
9. Bobyk, A., Kaminski, W. & Borzov, I. N. Gamow-Teller beta-decay strengths of neutron-deficient tin isotopes: comparison of FFST and pnBCS+QRPA results. *Acta Phys. Pol. B* **31,** 953–963 (2000).
10. Batist, L. *et al.* Systematics of Gamow-Teller beta decay "Southeast" of ^{100}Sn. *Eur. Phys. J. A* **46,** 45–53 (2010).
11. Schneider, R. *et al.* Production and identification of ^{100}Sn. *Z. Phys. A* **348,** 241–242 (1994).
12. Lewitowicz, M. *et al.* Identification of the doubly-magic nucleus ^{100}Sn in the reaction ^{112}Sn+^{nat}Ni at 63 MeV/nucleon. *Phys. Lett. B* **332,** 20–24 (1994).
13. Chartier, M. *et al.* Mass measurement of ^{100}Sn. *Phys. Rev. Lett.* **77,** 2400–2403 (1996).
14. Sümmerer, K. *et al.* Identification and decay spectroscopy of ^{100}Sn at the GSI projectile fragment separator FRS. *Nucl. Phys. A* **616,** 341–345 (1997).
15. Stolz, A. *et al.* Projectile fragmentation of ^{112}Sn at E_{lab} = 1A GeV. *Phys. Rev. C* **65,** 064603 (2002).
16. Bazin, D. *et al.* Production and beta-decay of rp-process nuclei ^{96}Cd, ^{98}In, and ^{100}Sn. *Phys. Rev. Lett.* **101,** 252501 (2008).
17. Geissel, H. *et al.* The GSI projectile fragment separator (FRS): a versatile magnetic system for relativistic heavy ions. *Nucl. Instrum. Methods B* **70,** 286–297 (1992).
18. Pietri, S. *et al.* Recent results in fragmentation isomer spectroscopy with rising. *Nucl. Instrum. Methods B* **261,** 1079–1083 (2007).
19. Plettner, C. *et al.* Beta decay of ^{100}In. *Phys. Rev. C* **66,** 044319 (2002).
20. Coraggio, L., Covello, A., Gargano, A. & Itaco, N. Structure of particle-hole nuclei around ^{100}Sn. *Phys. Rev. C* **70,** 034310 (2004).
21. Hamamoto, I. & Sagawa, H. Gamow-Teller beta decay and isospin impurity in nuclei near the proton drip line. *Phys. Rev. C* **48,** R960–R963 (1993).
22. Faestermann, T. *et al.* Decay studies of N ≈ Z nuclei from ^{75}Sr to ^{102}Sn. *Eur. Phys. J. A* **15,** 185–188 (2002).
23. Blazhev, A. *et al.* Observation of a core-excited E4 isomer in ^{98}Cd. *Phys. Rev. C* **69,** 064304 (2004).
24. Boutachkov, P. *et al.* High-spin isomers in ^{96}Ag: excitations across the Z = 38 and Z = 50, N = 50 closed shells. *Phys. Rev. C* **84,** 044311 (2011).
25. Cederwall, B. *et al.* Evidence for a spin-aligned neutron–proton paired phase from the level structure of ^{92}Pd. *Nature* **469,** 68–71 (2011).
26. Singh, B., Rodriguez, J. L., Wong, S. S. M. & Tuli, J. K. Review of log*ft* values in β-decay. *Nucl. Data Sheets (N.Y. N.Y.)* **84,** 487–563 (1998).

Supplementary Information is linked to the online version of the paper at www.nature.com/nature.

Acknowledgements We thank the staff of the GSI ion source and accelerator for the preparation of a stable, high-intensity ^{124}Xe beam, and we thank the fragment separator technicians for setting up the beamline detectors. We acknowledge discussions with G. Martínez-Pinedo, K. Langanke and A. Zuker. We are also grateful to the EUROBALL Owners Committee for the use of the Euroball Cluster Detectors. This work was supported by the BMBF under contracts 06MT238, 06MT9156, 06KY205I and 06KY9136I; by the GSI; by the DFG Cluster of Excellence 153 'Origin and Structure of the Universe'; by the EC within the FP6 through I3-EURONS (contract no. RII3-CT-2004-506065); and by the Swedish Research Council.

Author Contributions Fragment separator: H.W., P.B., H. Geissel, M.G., Zs.P. and C.N.; particle detectors: C.B.H., K. Straub, R.G., T.F., L.M. and F. Nebel; RISING γ-array: P.B., M.G., S.P., J.G., I.M.K. and H.-J.W.; data acquisition and analysis software: M.B., R.G., J.L.G., N.K. and L.M.; data analysis and interpretation: C.B.H., K. Straub, T.F., M.G., H. Grawe, R.K., K. Steiger, F. Nowacki and K. Sieja; shell model calculations: F. Nowacki and K. Sieja; writing of manuscript: C.B.H., T.F., R.G., H. Grawe, R.K., F. Nowacki and K. Sieja. All authors except H. Grawe, F. Nowacki and K. Sieja took part in the preparation and the experiments, and all authors commented on the final paper.

Author Information Reprints and permissions information is available at www.nature.com/reprints. The authors declare no competing financial interests. Readers are welcome to comment on the online version of this article at www.nature.com/nature. Correspondence and requests for materials should be addressed to T.F. (thomas.faestermann@ph.tum.de).